Year: 2016

Prolongation, deepening and warming of the metalimnion change habitat conditions of the harmful filamentous cyanobacterium Planktothrix rubescens in a prealpine lake

Yankova, Yana ; Villiger, Jörg ; Pernthaler, Jakob ; Schanz, Ferdinand ; Posch, Thomas

Abstract: The most prominent responses of Lake Zurich to climate warming include the increase of surface water temperatures, a reduced depth of spring mixing, and the persistent thriving of the harmful cyanobacterium Planktothrix rubescens, a low-light adapted species concentrating in the metalimnion during summer. To study changes of its habitat, we assessed the spatio-temporal metalimnetic boundaries by applying low-pass filtering and binary thresholding to temperature profiles of long-term data (1978–2013, weekly measurements). Due to increasing temperatures over the last 3.5 decades, the onset and duration of metalimnion formation changed significantly (stratification increased by 33 days). Moreover, the upper metalimnetic boundary has undergone a significant drawdown of 2.3 m, accounting for an overall decrease in metalimnion thickness. Being the most abundant species in this zone, P. rubescens was not negatively affected by altered temporal or spatial stratification patterns during its phase of net growth (July–September), as the zone of its optimal light-dependent buoyancy was still located within the metalimnion. The biomass of P. rubescens in August was even significantly related to increasing temperatures. Nevertheless, a further depression of the metalimnetic top boundary may eventually restrict P. rubescens by forcing it into layers of unfavourable light conditions or into the turbulent epilimnetic zone.

1 **Prolongation, deepening and warming of the metalimnion change habitat conditions of**

2 **the harmful filamentous cyanobacterium *Planktothrix rubescens* in a prealpine lake**

3 Yankova Yana, Villiger Jörg, Pernthaler Jakob, Schanz Ferdinand and Posch Thomas*

4 *Limnological Station, Department of Plant and Microbial Biology, University of Zurich,*

5 *Seestrasse 187, CH-8802 Kilchberg, Switzerland*

6

7 *Corresponding author: tel.: +41 44 63 49224, fax: +41 44 63 41225, email:

8 posch@limnol.uzh.ch

9

10

Abstract

The most prominent responses of Lake Zurich to climate warming include the increase of

surface water temperatures, a reduced depth of spring mixing, and the persistent thriving of

the harmful cyanobacterium *Planktothrix rubescens,* a low-light adapted species

concentrating in the metalimnion during summer. To study changes of its habitat, we assessed

the spatio-temporal metalimnetic boundaries by applying low-pass filtering and binary

thresholding to temperature profiles of long-term data (1978-2013, weekly measurements).

Due to increasing temperatures over the last 3.5 decades, the onset and duration of

metalimnion formation changed significantly (stratification increased by 33 days). Moreover,

the upper metalimnetic boundary has undergone a significant drawdown of 2.3 meter,

accounting for an overall decrease in metalimnion thickness. Being the most abundant species

in this zone, *P. rubescens* was not negatively affected by altered temporal or spatial

stratification patterns during its phase of net growth (July-September), as the zone of its

optimal light-dependent buoyancy was still located within the metalimnion. The biomass of *P.

rubescens* in August was even significantly related to increasing temperatures. Nevertheless, a

further depression of the metalimnetic top boundary may eventually restrict *P. rubescens* by

forcing it into layers of unfavourable light conditions or into the turbulent epilimnetic zone.

Keywords: lake warming, Lake Zurich, long-term data, metalimnion, neutral buoyancy,

Planktothrix rubescens

Introduction

Lakes are good reflectors of local aspects of climate change by having the characteristics of

enclosed ecosystems, and at the same time by being in dynamic exchange with the

atmosphere. Many studies of European lakes over the last decades have thus focused on

different aspects linked to climatic change. These included changes in thermal stratification

and mixing (Livingstone, 2003), oxygen content (Posch et al., 2012; North et al., 2014),

nutrient loading (Straile et al., 2003; O'Neil et al., 2012) and phytoplankton response

(Weyhenmeyer et al., 2002; Winder & Sommer, 2012). One of the most important issues

related to some of these changes is the large-scale occurrence of harmful algal and

cyanobacterial blooms (Johnk et al., 2008; Paerl & Huisman, 2008; Paerl et al., 2011).

The response of Lake Zurich (Switzerland) to climatic conditions has been extensively

investigated. It has been shown that warm winters have a positive effect on thermal stability,

and a negative impact on the spring mixing depth (Dokulil et al., 2006; Rempfer et al., 2010;

Posch et al., 2012). Livingstone (2003) has reported on the long-term increase of mean water

temperatures, on the prolongation of lake stratification and on the relationship between

climate warming and the reduced occurrence of complete water turnover (holomixis).

The most abundant primary producer in Lake Zurich is the toxic filamentous

cyanobacterium *Planktothrix rubescens* (Bossard et al., 2001). *P. rubescens* is a major part of

the phytoplankton community also in numerous other European lakes, including, e.g., Lake

Mondsee, Austria (Dokulil & Teubner, 2012), the Italian lakes Garda, Iseo and Como

(Salmaso et al., 2003; Salmaso, 2010), Lake Ammersee, Germany (Ernst et al., 2001), and

until recently, Lake Bourget, France (Jacquet et al., 2014). The present dominance of *P.*

rubescens in Lake Zurich was established during the re-oligotrophication period in the late

1970s (Supplementary Material, Fig. S1), characterised by reduced nutrient loadings

(Gammeter & Zimmermann, 2001) and severely changed nutrient stoichiometry (Posch et al.,

2012). Since then *P. rubescens* has been forming persistent reoccurring blooms of increasing

3

58   biomass, representing a potential hazard for humans and animals due to highly toxic

59   secondary metabolites such as microcystins (Blom et al., 2006).

60   This cyanobacterium is adapted to low light intensities, and, therefore, it is forced to

61   concentrate in the metalimnion (10-15 m) during the warm seasons (Supplementary Material,

62   Fig. S1). As long as there is a stable thermal stratification, the metalimnion as a habitat

63   guarantees saturating light conditions for cyanobacterial growth, and hampers the entrainment

64   of cyanobacteria into the turbulent epilimnetic zone. During summer, high irradiance in the

65   epilimnion would have a strong negative impact on this low-light adapted organism. *P.*

66   *rubescens* can regulate its vertical position in the water column, and buoyancy is provided by

67   intracellular gas vesicles, which allow a depth adjustment of 0.4 m d^{-1} (Walsby et al., 2001).

68   Thus, cyanobacteria can actively concentrate in the metalimnion during thermal stratification.

69   The critical collapse pressure of the gas vesicles is reached at approximately 80-90 m depth,

70   below which they are destroyed (Walsby et al., 1998). This aspect becomes of relevance in

71   spring, when holomixis transports cyanobacterial filaments into the deep hypolimnion. The

72   successful establishment of *P. rubescens* in many lakes is in large parts attributed to climate

73   warming: due to stabilisation of the thermal stratification and the reduced mixing depth, *P.*

74   *rubescens* loses less biomass during warm winters (Walsby et al., 1998; Posch et al., 2012).

75   Even though the characteristics and development of *P. rubescens* in Lake Zurich are

76   well studied, little is known about how climate warming influences its very habitat during

77   stable thermal stratification, i.e., the metalimnion, and if such changes potentially affect *P.*

78   *rubescens* population dynamics. In this study we used available long-term data of

79   cyanobacteria and physicochemical parameters to test the following three theses: (i)

80   Increasing water temperatures due to climate warming will affect the temporal and spatial

81   dynamics of the metalimnion in Lake Zurich; (ii) The expected earlier onset and temporal

82   extension of the metalimnion period is significantly related to the increasing biomass of *P.*

83   *rubescens;* (iii) Changes in the spatial dimensions and of other physical properties of the

84   metalimnion affect *P. rubescens* during its growth period in summer.

85

86   **Materials and Methods**

87   **Study site**

88   Lake Zurich (also referred to as Lower Lake Zurich) is a large (65 km^2, 30 km length), deep

89   (136 m), stratifying, prealpine lake located on the Swiss Plateau. It is well separated from the

90   fairly smaller Upper Lake Zurich by a sill, allowing for the inflow of only the upper 3 m of

91   surface water, and which is nevertheless the major inflow of Lake Zurich. The thermal regime

92   of the lake can be classified as generally monomictic with a water turn-over in early spring.

93   The lake undergoes holomixis after cold winters, whereas partial mixing (80-100 m) occurs

94   after mild winters (Posch et al., 2012). In late autumn, thermal stratification of the upper

95   water body gets eroded, which leads to a turbulent mixed zone between 0-30 m. Lake Zurich

96   is an important freshwater reservoir for over 1 million people. Over the past century the lake

97   has been exposed to regular monitoring and management, involving a re-oligotrophication

98   process with reduced phosphorus deposition starting in the 1950s, improved waste water

99   treatment, inflow and outflow control. For further limnological information and a map of the

100   lake we refer to Garneau et al. (2013).

101

102   **Long-term data**

103   Data of water temperature and photosynthetically active radiation have been collected weekly

104   near the deepest point of Lake Zurich (N 47° 17.147, E 8° 35.460; 406 m a.s.l. at surface) for

105   the period of 1978 to 2013. In total, 1517 temperature profiles (0-20 m, unless otherwise

106   stated) were measured at 1 m intervals using a TTM 72 thermistor thermometer (Züllig AG,

107   Rheineck, Switzerland) between 1978 and 2008, and a YSI multiprobe (Yellow Springs

108   Instruments 6600) from 2008 onward. Underwater light profiles were determined with a

109   spherical quantum sensor (LI-Cor) for the period of 1985 to 2013 at the same spatial and

110   temporal resolution as temperature measurements. A dataset of monthly *P. rubescens* biomass

111   profiles (0, 1, 2.5, 5, 7.5, 10, 12.5, 15, 20, 30, 40, 80, 120, 135 m), measured also at the

112   deepest point of the lake (136 m) between 1972 and 2011, was provided by the City of Zurich

113   Water Supply Company (Supplementary Material, Fig. S1). Air temperature analysis for the

114   corresponding study period (1978-2013) is based on monthly averages provided by the

115   Federal Office of Meteorology and Climatology MeteoSwiss measured in Zurich-Fluntern (N

116   47° 22.7, E 8° 33.9; 556 m a.s.l.). The meteorological station is located in a distance of 10 km

117   north of the deepest point (sampling point), and 2.8 km from the northern end (major outflow)

118   of Lake Zurich.

119

120   **Determination of the boundaries and duration of the metalimnion**

121   The metalimnion of lakes is defined as the zone with the steepest thermal gradient (usually Δ

122   0.5 - 4.5 °C m^{-1}), thereby forming a physical barrier for mixing between surface and deep

123   water layers. Its formation in spring, caused by the progressive warming of surface waters,

124   can be described as a dynamic process. Sudden cooling events in this time of the year often

125   lead to a disruption of the metalimnion followed by re-stabilization. This makes the

126   determination of an exact time point of metalimnion formation especially challenging. We

127   compared two different years to illustrate this problem (Fig. 1). To define spatial and temporal

128   boundaries of the metalimnion, the two dimensional (time, depth) temperature profiles were

129   low-pass filtered with a linear kernel (size = 3 × 3) to remove extreme transitions between

130   sampling points and short timed effects. Subsequently, the coherent area which covered a

131   maximum of data points with a temperature gradient of $\geq$ 0.5 °C m^{-1} was defined as the

132   metalimnion (Fig. 1). The definite starting and ending dates were determined by linear

133   interpolation between the adjacent weekly sampling dates. The duration of the metalimnetic

134   stratification was determined as the difference between the last and the first date (in Julian

135   day) of metalimnion formation for each year. Metalimnion thickness was defined as the

136   difference between the lower and the upper depth boundary, and its center was calculated as

137   the mean of these boundaries.

138

139   **Data treatment**

140   Serial correlation of the residuals of time series can significantly affect trend estimates (von

141   Storch, 1995), thus it has to be eliminated. For each set of monthly averaged air and water

142   temperatures, as well as metalimnion spatial and temporal data we applied the "trend-free pre-

143   whitening" (TFPW) procedure proposed by Yue et al. (2002). This method first evaluates the

144   presence of a trend by assessing if the trend slope b is close to zero (no trend) or not

145   (assumption for a linear trend). If a trend is detected, it is subtracted from the data. Significant

146   autocorrelations at lag 1 of the detrended series are then removed. Subsequently, the trend is

147   re-added to the pre-whitened series. Following this, adjusted Mann Kendall (MK) *tau*

148   coefficients, *p*-values and Sen's slopes (Sen, 1968) of the autocorrelation-free data are

149   estimated. The overall trends in air temperature, as well as trends of water temperature for

150   each depth (0-20 m) over the whole study period (1978-2013) were analyzed with MK

151   seasonal trend tests due to the presence of strong reoccurring annual patterns. Serial

152   dependence was taken into account according to Hirsch & Slack (1984).

153   The magnitude of significant changes in the studied parameters over time was

154   calculated using the linear regression equation $Y = b \cdot X + a$, with Y being the predicted value

155   (e.g., temperature), b the Sen's slope of the regression line, X the predictor (e.g., year), and 'a'

156   the intercept of Sen's slope. Based on this equation we determined the Y values for the years

157   X=1978 and X=2013, and calculated, e.g. the temperature increase, as the difference between

158   Y_{2013} and Y_{1978}.

159   Spearman's correlation test was used to test for significant correlations between *P.*

160   *rubescens* biomass and metalimnion spatial and temporal dimensions, as well as between

161   biomass and neutral buoyancy depth.

162   Linear regression was applied to assess the relationship between the biomass of

163   metalimnetic *P. rubescens* populations in summer, as well as between these populations and

164   the temperature of metalimnion center. The residuals from the linear model were tested for

165   normality and significant serial dependence using the autocorrelation- and partial

166   autocorrelation functions. No significant autocorrelations were detected for this data.

167   Schmidt stability is defined as the energy per unit area required for mixing without

168   input or loss of heat in lakes (Idso, 1973; Schmidt, 1928). For a comparison with our

169   metalimnion determination approach, we estimated Schmidt stability for each temperature

170   profile only for the zone of 0-20 m, which corresponds to the epi- and metalimnion in Lake

171   Zurich. Estimation of the energy required to mix the whole water column down to 136 m, as

172   already shown by Livingstone (2003), would give information about potential full turn-over,

173   which is outside the scope of this study. Furthermore, in the last decade the mixing depth in

174   Lake Zurich has rarely exceeded 130 m (Posch et al., 2012). Stratification start and end points

175   were estimated based on several Schmidt stability thresholds (10-150 J m^{-2}) for each year of

176   the period 1978-2013, after linear interpolation of calculated values.

177   *P. rubescens* biomass (*BPr*, in µg L^{-1} fresh weight) was first linearly interpolated to

178   achieve a vertical resolution of 1 m intervals. The total biomass (in tons) of a depth layer (*z*)

179   was calculated by multiplying BPr_z with the total water volume of this layer (V_z, in m^3). Total

180   epilimnetic biomass (in tons) was calculated with the following equation:

181     $$Total\ epilimnetic\ biomass\ (tons) = \sum_{z=0}^{20} BPr_z \times V_z$$

182   The water volume for $z = 0$ m (V_0) comprised the surface layer from 0 m to 0.5 m. For all

183   other water layers ($z = 1$-20 m), volumes for a defined depth z comprised the zone of 0.5 m

8

184 above and below z (e.g., V_1 = water volume between 0.5-1.5 m). The annual population

185 minimum of *P. rubescens* in June also represents the start of its seasonal growth period,

186 which ends with the annual population maximum in November.

187 Neutral buoyancy depth was defined after Walsby et al. (2004) as the depth with an

188 irradiance level at which 50 % of *P. rubescens* filaments float, i.e., 6.51 µmol m^{-2} s^{-1}. This

189 depth was estimated by cubic spline interpolation of the underwater light attenuation curves.

190 Data interpolation, statistical analyses and Schmidt stability calculations were

191 performed using the software R. TFPW was computed using the package 'zyp'. For MK

192 seasonal trend test we chose the package 'EnvStats'. Schmidt stability was calculated using

193 the package 'rLakeAnalyzer'. Bray-Curtis dissimilarity indices were calculated with the add-

194 in software XLSTAT (Addinsoft^{TM}) in Excel.

Results

Long-term trends in air temperatures for the period 1978-2013

MK trend tests for discrete months showed highly significant increases in air temperatures for the spring months (April: *tau* = 0.44, *p* < 0.001; May: *tau* = 0.33, *p* < 0.01; June: *tau* = 0.36, *p* < 0.01, *n* = 36 for each month) and for November (*tau* = 0.27, *p* < 0.05, *n* = 36). Air temperatures in all other months showed positive trends (except for December) but no statistically significant time trends (Fig. 2, Supplementary Material, Fig. S2). Nevertheless, overall air temperature for the same period increased significantly by 1.5 °C (seasonal MK: *tau* = 0.2, *p* < 0.001, *n* = 432; Fig. 2). The most pronounced rise in air temperature was in April, May, and June (3.2 °C, 2.4 °C and 2.5 °C), and these months predominantly accounted for the overall trend. The alternating occurrence of colder and warmer years appeared to interfere with any long-term trend of temperature during the winter months (December to February; Supplementary Material, Fig. S2).

Thermal characteristics of the water column

In parallel with air temperature trends, the water column of Lake Zurich exhibited distinct changes in thermal structure. Local air temperature dynamics are closely linked to changes in the thermal properties of surface layers in lakes (Livingstone, 2003; Straile et al., 2003; Dokulil, 2014).

An in-depth analysis of the long-term monthly averages per depth layer did not only reveal a significant temperature increase in the upper 5 m of the water column in several months, but also a large-scale, yet uneven, warming pattern across the whole upper water column (0-20 m, Fig. 2). In contrast to air temperature, where significant trends were only observed for four months, water temperatures significantly increased from March until December at certain depths. In spring (April to June), surface layers showed significant temperature increase, affecting the water column even down to 14 m in June. From July on,

221   lake warming was restricted to deeper layers, and in October significant trends could be only

222   determined for the water column between 10 and 15 m (Fig. 2). In November a warming of

223   the surface, and from 4-17 m depth was observed, which reflects both, the increase in air

224   temperature and the erosion of the epi- and metalimnetic stratification. As the significant air

225   temperature increase in November seemed to affect only the surface, a possible heat transfer

226   from the former metalimnion into surrounding water layers is very likely. The lack of

227   significant air temperature increase in December contradicts the water temperature increase in

228   0-20 m observed in this month, which could also be an indication for distribution of heat from

229   deeper layers.

230   Trend analyses calculated per depth and for the full year showed a homogenous

231   warming of the surface water body between 0 to 15m during the last 36 years (Fig. 2, overall

232   trends). Overall, the water temperature increased by up to 1.4 °C in 7-9 m (seasonal MK,

233   each: *tau* = 0.3, *p* < 0.001, *n* = 432).

234   The maximum increase per depth on the surface (0-4 m) was found in May (Fig. 2,

235   right panel). With increasing depth (4-12 m) maximal increases were observed in July and

236   August. The strongest rise in water temperature per depth were recorded for July in 6 m and 7

237   m depth (max. 4.13 °C for both; Fig. 2, right two panels). In deeper layers maximal

238   temperature rises were recorded in October (13-15 m) and December (16-17 m).

239   Additionally, the increase in water temperature seemed to be more pronounced than

240   that in air temperature over time. A comparison between the Sen's slopes of water and air

241   temperatures for each month and depth revealed higher values of the former at several depths

242   in May and June (Supplementary Material, Fig. S3).

243

Temporal changes of metalimnion dynamics

245   The metalimnion determination highlighted significant changes of temporal dimensions in

246   Lake Zurich (Fig. 3). Onset and duration of metalimnion appearance showed significant

247   trends over the total period (Fig. 3a). Stratification onset denoted a preponed shift of 17 days

248   (MK: *tau* = -0.32, *p* < 0.01, *n* = 36), whereas stratification end exhibited no significant trend

249   between 1978 and 2013. Duration of metalimnion appearance, however, was extended by 33

250   days over the study period (MK: *tau* = 0.36, *p* < 0.01, *n* = 36; Fig. 3b).

251   The constant shift towards an earlier onset propagated clearly through decades. In the

252   first decade, 75 % of metalimnion formation started in May, and 25 % in April. In the second

253   decade, 60 % of onsets occurred in April, and 40 % in May. During the last decade, 43 % of

254   metalimnion onsets were in April, 43 % in May, and 14 % already in March. In addition, 63

255   % of the years with duration > 200 days were found in the third decade, whereas 75 % of the

256   years with shortest duration (< 170 days) fell into the first one.

257

258   **Comparison of metalimnion detection and Schmidt stability**

259   Onset, end and duration of the metalimnion for each year were compared to equivalent values

260   of annual stratification stability determined by Schmidt stability analysis with thresholds

261   ranging between 10 and 150 J m^{-2} (Supplementary Material, Fig. S4). The best agreement

262   between the two approaches was found at a threshold of 110 J m^{-2} for onset and duration (R^2 >

263   0.7). The agreement between Schmidt stability and metalimnion end were considerably lower

264   (R^2 = 0.3) and comparable results were achieved with thresholds between 30-110 J m^{-2}.

265

266   **Spatial dynamics of the metalimnion**

267   Analyses for each month during metalimnion appearance showed that in July and August, the

268   top boundary exhibited a significant lowering by 2.3 m and 1.2 m, respectively (MK, each:

269   *tau* = 0.3, *p* < 0.05, *n* = 36) between 1978 and 2013 (Fig. 4a). The development of the lower

270   boundary showed a significant increase by 2 m (MK, *tau* = 0.4, *p* < 0.05, *n* = 28) in

271   November and no trend for the rest of the year (Fig. 4b).

272   Metalimnion thickness is determined as difference between its lower and upper

273   boundaries. The metalimnion underwent a significant decrease in thickness by 2.8 m in July

274   (MK, *tau* = -0.4, $p < 0.001$, $n = 36$) and by 1.8 m in August (MK, *tau* = -0.4, $p < 0.01$, $n = 36$)

275   over the studied period (Fig. 4c). By contrast, it exhibited a significant increase in thickness

276   by 2 m in November in the same period (MK, *tau* = 0.4, $p < 0.01$, $n = 28$). The MK trend

277   analysis for average metalimnion thickness in July and August indicated a clear loss of

278   thickness by 2.4 m during the last 36 years (Fig. 4d).

279

280   **Impact of metalimnion changes on the occurrence of *P. rubescens***

281   Our thesis that longer metalimnion duration would have a positive influence on *P. rubescens*

282   development could not be verified. There was no significant correlation between the

283   population maximum of *P. rubescens* (tons lake^{-1}) in November and metalimnion duration

284   (Table 1). However, a significant correlation was found between the start population size of

285   *P. rubescens* and stratification onset (Table 1), i.e., years with early metalimnion formations

286   (in Julian days) were also characterized by larger cyanobacterial biomasses already in spring.

287   Thus, shorter water turnovers during the winter months favored the survival of *P. rubescens*

288   populations (Posch et al., 2012). This effect seemed to propagate throughout the season, as we

289   found also a significant correlation between metalimnion onset (in Julian days) and *P.*

290   *rubescens* biomasses in November (Table 1).

291   We also assessed possible effects of metalimnion changes on the development of *P.*

292   *rubescens* during its growth phase. The depth of population maxima (μg fresh-weight L^{-1}) in

293   June was significantly correlated with the neutral buoyancy depth (Spearman's *rho* = 0.49, *p*

294   < 0.05), but not with the boundaries of the metalimnion (Fig. 5, Supplementary Material, Fig.

295   S5). In July the depth of maximum biomass correlated with the center of the metalimnion

296   (Spearman's *rho* = 0.38, $p < 0.05$), and the majority of *P. rubescens* remained within the

297   boundaries of neutral buoyancy. This was also true for the situation in August. In September

298   the depths of both *P. rubescens* maxima and neutral buoyancy shifted toward the upper

299   boundary of the metalimnion (Fig. 5; Supplementary Material, Fig. S5). Regression analysis

300   indicated that the biomass of *P. rubescens* in the metalimnion during the summer months was

301   strongly determined by the biomass of the previous month (July-June: p < 0.001; August-July:

302   p < 0.001; Fig. 6a,b). In addition, the biomass in August was also significantly related to the

303   temperature of the metalimnetic center (p < 0.001; Fig. 6d), where we also observed a

304   significant long-term increase of water temperatures (Fig. 6f). However, these trends were not

305   observed for the month July (Fig. 6c,e).

Discussion

Impact on climate warming on metalimnion temporal dynamics

So far changes of air temperature have been typically analysed at seasonal, annual or decadal resolution in limnological studies (Livingstone, 2003; Blenckner et al., 2007; Dokulil et al., 2010). A more in-depth analysis, however, shows the contribution of particular months to overall trends. For the region of Lake Zurich we found strongest air temperature increases in spring (April to June) and in November. Increase of air temperature particularly in spring can be crucial for establishing thermal stability and for timing of metalimnion onset in a lake. This is important as a weak thermal stratification can often be disrupted by weather-induced internal waves in spring (Bleiker & Schanz, 1997). It has been shown that air temperature is a reliable forcing factor reflecting climate warming, which can significantly influence the heat balance of lakes (Sweers, 1976; Rempfer et al., 2010). Our analysis considered only temperature changes based on links between external warming and lake warming. However, other factors involved in the thermal budget of Lake Zurich, such as heat fluxes via inflows and outflows, and precipitation have been shown to be rather negligible for the total heat balance of the lake (Imboden & Wüest, 1995).

We document a clear progression of metalimnion onset in Lake Zurich from May to April and March, respectively, between 1978 and 2013. Similar shifts in onset timing were also found for Müggelsee, Germany (Shatwell et al., 2008). Moreover, the earlier onset rather than the later termination was primarily (significantly) responsible for the observed prolongation of the metalimnion period. This is consistent with results from other studies on stratification dynamics in lakes of the Northern Hemisphere. Winder & Schindler (2004) reported on the importance of an earlier onset for the prolongation of stratification in Lake Washington, USA. Dokulil (2014) also highlighted the important contribution of a shifted onset to the length of stratification in Lake Mondsee, Austria. Both studies reported a prolongation of the stratification by > 25 d, which is in agreement with the overall extension

15

332 of 33 d found for Lake Zurich between 1978 and 2013. Our results also confirm the findings

333 of Livingstone (2003), who reported on a stratification extension of up to 3 weeks based on a

334 50 years data set of Lake Zurich. However, we could not confirm the decisive role of

335 stratification ending for this prolongation, as it was suggested in that study.

336   The water column in Lake Zurich underwent a significant but uneven large-scale

337 temperature increase during the studied period. The warming of the upper layers in spring and

338 summer subsequently shifted downwards and mainly seemed to affect the metalimnion in

339 September and October. Interestingly, the strongest annual increase in water temperature was

340 found in or close to the metalimnetic zone. Furthermore, water temperature increases in May,

341 July and August partially exceeded even the strongest increase in air temperature found in

342 April (Supplementary Material, Fig. S3). Discrepancy in temperature increase of water versus

343 air associated with reduced lake cooling has also been documented in the surface waters of

344 Lake Superior, USA (Austin & Colman, 2007) during the summer months.

345   Water temperature increases in November and December were detected for nearly the

346 whole water body (4-17 m and 0-20 m, respectively). However, the significant rise in air

347 temperature in November seemed to affect only the surface (0 m) water temperature in this

348 month. These findings lead us to hypothesize that strong air temperature increase in spring

349 causes an accumulation of thermal energy in the metalimnion. Once a stable metalimnion is

350 formed in late spring/early summer, the storage of heat in the following months (July-

351 September) is rather unaffected by cooling events and turbulent heat exchange (Wuest &

352 Lorke, 2003). Starting from November, when the physical separation between epi- and

353 metalimnion gets eroded due to autumnal surface mixing, a dispersal of thermal energy from

354 the former metalimnion into the mixed zone is very likely.

355

356 **Comparison of Schmidt stability estimations and metalimnion detection approach**

357 Assessing the spatial development of the metalimnion requires a good resolution of water

358 temperature profiles. Hence, many studies on the specifics of thermal stratification involve

359 modelling approaches (Peeters et al., 2002; 2007), or Schmidt stability estimations (Straile et

360 al., 2003; Rempfer et al., 2010). Schmidt stability exactly defines the stability of the water

361 column based on density gradients, however, it does not inform about the spatial structure of

362 stratification within a lake, i.e. about the division in epi-, meta-, and hypolimnion.

363   Metalimnion is per definition the zone with the steepest thermal gradients per depth,

364 thus, we based our approach on gradient detection. We applied a technique known from

365 image analysis, two-dimensional linear smoothing (low-pass kernel) followed by binary

366 thresholding and detection of the largest coherent area. This approach overcomes the possible

367 difficulties of estimating metalimnion boundaries due to unstable stratification phases caused

368 by short-term weather changes (Fig. 1). At the same time, this method allowed for a depiction

369 of the metalimnion as a dynamic entity and the assessment of its shape.

370   In terms of temporal dynamics, our approach of metalimnion detection agrees well

371 with stratification estimations by Schmidt stability, if both analyses were conducted for the

372 upper 20 m. Livingstone (2003) estimated a threshold of ≥ 200 J m^{-2} for stratification onset

373 and ≤ 200 J m^{-2} for stratification termination considering the whole water column in Lake

374 Zurich. Since we limited our analysis to the upper water layers (0-20m), this threshold cannot

375 be applied in our case. We thus conducted a series of analyses with varying Schmidt stability

376 thresholds, which resulted in maximal agreement between both methods at 110 J m^{-2}

377 (Supplementary Material, Fig. S4).

378

379 **Changing spatial structures of the metalimnion in Lake Zurich**

380 The pronounced lowering of the upper metalimnion boundary (Fig. 4) in summer in Lake

381 Zurich suggests a direct effect of the strong temperature increase in spring, leading to

382 subsequent greater stratification stability and enlargement of the epilimnion. More stable

383   conditions could influence the food web of lakes through enhancing niche separation and

384   providing refuge zones for zooplankton (Teubner et al., 2003; Guilizzoni et al., 2012;

385   Gauthier et al., 2014). Moreover, the deepening of the upper boundary in July and August

386   accounts for the overall decrease in metalimnion thickness over the whole period. The local

387   increase in metalimnion thickness observed in November was most likely related to the

388   prolongation of the stratification, which led to a more pronounced presence of a metalimnion

389   in this month.

390

391   **Context between changing metalimnion dynamics and *P. rubescens***

392   We explored the thesis that *P. rubescens* might be affected by climate warming induced long-

393   term changes of the metalimnion. Recently Posch et al. (2012) showed that the depth of

394   spring turnover has a crucial effect on the subsequent annual population of *P. rubescens* in

395   Lake Zurich. The yearly population growth of these cyanobacteria commences in June and

396   they reach highest concentrations in November. Hence, the magnitude of biomass which

397   survives the cold winter and spring mixis seems to be decisive for the total population size in

398   the subsequent year. Since climate change has altered Lake Zurich mixing regime towards a

399   more frequent occurrence of years with insufficient spring mixis, *P. rubescens* has been able

400   to form larger annual populations with steady increasing biomass over the last years.

401   In addition to these observations, we expected that the trend of increasing metalimnion

402   duration and changes in its thickness might also have an influence on the success of *P.*

403   *rubescens* in Lake Zurich. However, the expanded metalimnion duration does not seem to

404   significantly affect the population maxima of *P. rubescens* found in November. Indeed, the

405   thermal stratification in Lake Zurich occasionally lasts until mid-November. Nevertheless, in

406   October and November *P. rubescens* is distributed over the upper 20 m of the water column

407   as it gets entrained in epilimnetic layers due to instable weather conditions (Van den

408   Wyngaert et al., 2011). Therefore, the presence of the metalimnion at this time of the year can

409 be considered of little importance for cyanobacteria. In addition, in November the

410 metalimnion reaches greater depths (14-19 m in average) with limiting light intensities even

411 for a low-light adapted species such as *P. rubescens*. Indeed, *P. rubescens* moves to the upper

412 boundary of the metalimnion already in September due to light limitation in deeper zones

413 (Fig. 5).

414   Instead, the correlation of both, the start and end population of *P. rubescens* with the

415 metalimnion onset (Table 1), suggests that earlier formation is much more relevant for

416 population size than its termination. In addition, the correlation between population maximum

417 and decreasing average metalimnion thickness (Table 1) indicates that the reduced habitat size

418 is not (yet) a limiting factor for *P. rubescens* growth.

419   The strong context between biomass maxima and neutral buoyancy depth in June

420 clearly shows the behavioural adaptation of the *P. rubescens* population to still variable light

421 conditions during the initial phase of metalimnion formation. The cyanobacterium regulates

422 its depth within this zone through buoyancy according to daily insolation (Walsby et al.,

423 2001). Therefore, in the summer months (July-August), when the stratification in the lake is

424 stable, *P. rubescens* maxima are located in the zone of neutral buoyancy (Supplementary

425 Material, Fig. S5). This was already documented in previous studies showing close similarity

426 between neutral buoyancy depth and *P. rubescens* maxima during summer stratification

427 (Walsby & Schanz, 2002; Walsby et al., 2004). Although the reduction of its habitat size did

428 not seem to affect *P. rubescens* in July, it is nevertheless related to the depth of optimal

429 buoyancy: While the upper metalimnetic boundary decreased, the depth of neutral buoyancy -

430 exclusively related to ambient light conditions- did not change over time. This suggests that

431 the optimal zone for *P. rubescens* may come critically close to the mixed layer with

432 progressing lake warming. In September, both *P. rubescens* maxima and neutral buoyancy

433 depth were in critical vicinity to the upper boundary of the metalimnion (Fig. 5,

434 Supplementary Material, Fig. S5).

435   The main factor influencing *P. rubescens* biomass in summer was the biomass of the

436   preceding month. However, regression analysis revealed that temperature of the central

437   metalimnetic layer was also significantly correlated with cyanobacterial biomass, albeit only

438   in August. The average temperature of the metalimnion centre for July was 13 ± 1 °C between

439   1978 and 2013. The temperature in the centre did not increase significantly in July, but we

440   documented a long-term warming from 11.8 °C to 14.3 °C in August. Experiments with *P.*

441   *rubescens* cultures have shown that the growth rate increases with temperature, to a maximum

442   at 25 °C (Davis & Walsby, 2002; Oberhaus et al., 2007). Our findings, therefore, strongly

443   suggest that the warming of the metalimnion in late summer might have a positive effect on

444   the growth of *P. rubescens* at the rather stable optimal light (neutral buoyancy) conditions

445   during this period.

446

447   **Conclusion**

448   Our study identified significant shifts in onset and duration of the metalimnion and, moreover,

449   suggests an important role of this zone for transient heat storage in Lake Zurich. There are

450   indications that the compression and deepening of the metalimnion in late summer may

451   eventually restrict *P. rubescens* by forcing it into layers of unfavourable light conditions or

452   into the turbulent epilimnetic zone. However, the earlier onset and higher metalimnetic

453   temperatures might so far have more than counterbalanced potential negative effects as both

454   factors appear to favour the growth of *P. rubescens* in the studied system.

455

References

Austin, J. A. & S. M. Colman, 2007. Lake Superior summer water temperatures are increasing more rapidly than regional air temperatures: A positive ice-albedo feedback. Geophysical Research Letters 34.

Bleiker, W. & F. Schanz, 1997. Light climate as the key factor controlling the spring dynamics of phytoplankton in Lake Zurich. Aquatic Sciences 59:135-157.

Blenckner, T., R. Adrian, D. M. Livingstone, E. Jennings, G. A. Weyhenmeyer, D. G. George, T. Jankowski, M. Jarvinen, C. N. Aonghusa, T. Nõges, D. Straile & K. Teubner, 2007. Large-scale climatic signatures in lakes across Europe: a meta-analysis. Global Change Biology 13:1314-1326.

Blom, J. F., H. I. Baumann, G. A. Codd & F. Jüttner, 2006. Sensitivity and adaptation of aquatic organisms to oscillapeptin J and D-Asp(3),(E)-Dhb(7) microcystin-RR. Archiv Für Hydrobiologie 167:547-559.

Bossard, P., S. Gammeter, C. Lehmann, F. Schanz, R. Bachofen, H. R. Bürgi, D. Steiner & U. Zimmermann, 2001. Limnological description of the Lakes Zurich, Lucerne, and Cadagno. Aquatic Sciences 63:225-249.

Davis, P. A. & A. E. Walsby, 2002. Comparison of measured growth rates with those calculated from rates of photosynthesis in *Planktothrix* spp. isolated from Blelham Tarn, English Lake District. New Phytologist 156:225-239.

Dokulil, M. T., 2014. Impact of climate warming on European inland waters. Inland Waters 4:27-40.

Dokulil, M. T., A. Jagsch, G. D. George, O. Anneville, T. Jankowski, B. Wahl, B. Lenhart, T. Blenckner & K. Teubner, 2006. Twenty years of spatially coherent deepwater warming in lakes across Europe related to the North Atlantic Oscillation. Limnology and Oceanography 51:2787-2793.

Dokulil, M. T. & K. Teubner, 2012. Deep living *Planktothrix rubescens* modulated by environmental constraints and climate forcing. Hydrobiologia 698:29-46.

Dokulil, M. T., K. Teubner, A. Jagsch, U. Nickus, R. Adrian, D. Straile, T. Jankowski, A. Herzig & J. Padisak, 2010. The Impact of Climate Change on Lakes in Central Europe. In George, G. [ed], Impact of Climate Change on European Lakes. Aquatic Ecology Series: 387-409.

Ernst, B., B. Hitzfeld & D. Dietrich, 2001. Presence of *Planktothrix* sp and cyanobacterial toxins in Lake Ammersee, Germany and their impact on whitefish (*Coregonus lavaretus* L.). Environmental Toxicology 16:483-488.

498   Gammeter, S. & U. Zimmermann, 2001. Changes in phytoplankton productivity and

499   composition during reoligotrophication in two Swiss lakes. Verhandlungen der

500   Internationalen Vereinigung für Theoretische und Angewandte Limnologie 27:2190-2193.

501   Garneau, M.-È., T. Posch, G. Hitz, F. Pomerleau, C. Pradalier, R. Siegwart & J. Pernthaler,

502   2013. Short-term displacement of *Planktothrix rubescens* (cyanobacteria) in a pre-alpine

503   lake observed using an autonomous sampling platform. Limnology and Oceanography

504   58:1892-1906.

505   Gauthier, J., Y. T. Prairie & B. E. Beisner, 2014. Thermocline deepening and mixing alter

506   zooplankton phenology, biomass and body size in a whole-lake experiment. Freshwater

507   Biology 59:998-1011.

508   Guilizzoni, P., S. N. Levine, M. Manca, A. Marchetto, A. Lami, W. Ambrosetti, A. Brauer, S.

509   Gerli, E. A. Carrara, A. Rolla, L. Guzzella & D. A. L. Vignati, 2012. Ecological effects of

510   multiple stressors on a deep lake (Lago Maggiore, Italy) integrating neo and

511   palaeolimnological approaches. Journal of Limnology 71:1-22.

512   Hirsch, R. M. & J. R. Slack, 1984. A Nonparametric Trend Test for Seasonal Data with Serial

513   Dependence. Water Resources Research 20:727-732.

514   Idso, S. B., 1973. Concept of lake stability. Limnology and Oceanography 18:681-683.

515   Imboden, D. M. & A. Wüest, 1995. Mixing mechanisms in lakes. In Lerman, A., D. M.

516   Imboden & J. R. Gat [eds], Physics and chemistry of lakes, 2nd ed Springer: 83–138.

517   Jacquet, S., O. Kerimoglu, F. Rimet, G. Paolini & O. Anneville, 2014. Cyanobacterial bloom

518   termination: the disappearance of *Planktothrix rubescens* from Lake Bourget (France) after

519   restoration. Freshwater Biology 59:2472-2487.

520   Johnk, K. D., J. Huisman, J. Sharples, B. Sommeijer, P. M. Visser & J. M. Stroom, 2008.

521   Summer heatwaves promote blooms of harmful cyanobacteria. Global Change Biology

522   14:495-512.

523   Livingstone, D. M., 2003. Impact of secular climate change on the thermal structure of a large

524   temperate central European lake. Climatic Change 57:205-225.

525   North, R. P., R. L. North, D. M. Livingstone, O. Köster & R. Kipfer, 2014. Long-term

526   changes in hypoxia and soluble reactive phosphorus in the hypolimnion of a large

527   temperate lake: consequences of a climate regime shift. Global Change Biology 20:811-

528   823.

529   O'Neil, J. M., T. W. Davis, M. A. Burford & C. J. Gobler, 2012. The rise of harmful

530   cyanobacteria blooms: The potential roles of eutrophication and climate change. Harmful

531   Algae 14:313-334.

532 Oberhaus, L., J. F. Briand, C. Leboulanger, S. Jacquet & J. F. Humbert, 2007. Comparative

533   effects of the quality and quantity of light and temperature on the growth of *Planktothrix*

534   *agardhii* and *P. rubescens*. Journal of Phycology 43:1191-1199.

535 Paerl, H. W., N. S. Hall & E. S. Calandrino, 2011. Controlling harmful cyanobacterial blooms

536   in a world experiencing anthropogenic and climatic-induced change. Science of the Total

537   Environment 409:1739-1745.

538 Paerl, H. W. & J. Huisman, 2008. Climate - Blooms like it hot. Science 320:57-58.

539 Peeters, F., D. M. Livingstone, G. H. Goudsmit, R. Kipfer & R. Forster, 2002. Modeling 50

540   years of historical temperature profiles in a large central European lake. Limnology and

541   Oceanography 47:186-197.

542 Peeters, F., D. Straile, A. Lorke & D. M. Livingstone, 2007. Earlier onset of the spring

543   phytoplankton bloom in lakes of the temperate zone in a warmer climate. Global Change

544   Biology 13:1898-1909.

545 Posch, T., O. Köster, M. M. Salcher & J. Pernthaler, 2012. Harmful filamentous

546   cyanobacteria favoured by reduced water turnover with lake warming. Nature Climate

547   Change 2:809-813.

548 Rempfer, J., D. M. Livingstone, C. Blodau, R. Forster, P. Niederhauser & R. Kipfer, 2010.

549   The effect of the exceptionally mild European winter of 2006-2007 on temperature and

550   oxygen profiles in lakes in Switzerland: A foretaste of the future? Limnology and

551   Oceanography 55:2170-2180.

552 Salmaso, N., 2010. Long-term phytoplankton community changes in a deep subalpine lake:

553   responses to nutrient availability and climatic fluctuations. Freshwater Biology 55:825-

554   846.

555 Salmaso, N., G. Morabito, R. Mosello, L. Garibaldi & M. Simona, 2003. A synoptic study of

556   phytoplankton in the deep lakes south of the Alps (lakes Garda, Iseo, Como, Lugano and

557   Maggiore). Journal of Limnology 62:207-227.

558 Schmidt, W., 1928. Über die Temperatur- und Stabilitätsverhältnisse von Seen. Geografiska

559   Annaler 10:145-177.

560 Sen, P. R., 1968. Estimates of the Regression Coefficient Based on Kendall's Tau. Journal of

561   the American Statistical Association 63:1379-1389.

562 Shatwell, T., J. Kohler & A. Nicklisch, 2008. Warming promotes cold-adapted phytoplankton

563   in temperate lakes and opens a loophole for Oscillatoriales in spring. Global Change

564   Biology 14:2194-2200.

565 Straile, D., K. Johnk & H. Rossknecht, 2003. Complex effects of winter warming on the

566   physicochemical characteristics of a deep lake. Limnology and Oceanography 48:1432-

567   1438.

568 Sweers, H. E., 1976. Nomogram to Estimate Heat-Exchange Coefficient at Air-Water-

569   Interface as a Function of Wind Speed and Temperature - Critical Survey of Some

570   Literature. Journal of Hydrology 30:375-401.

571 Teubner, K., M. Tolotti, S. Greisberger, H. Morscheid, M. T. Dokulil & H. Morscheid, 2003.

572   Steady state phytoplankton in a deep pre-alpine lake: species and pigments of epilimnetic

573   versus metalimnetic assemblages. Hydrobiologia 502:49-64.

574 Van den Wyngaert, S., M. M. Salcher, J. Pernthaler, M. Zeder & T. Posch, 2011. Quantitative

575   dominance of seasonally persistent filamentous cyanobacteria (*Planktothrix rubescens*) in

576   the microbial assemblages of a temperate lake. Limnology and Oceanography 56:97-109.

577 von Storch, V., 1995. Misuses of statistical analysis in climate research. In von Storch, H. &

578   A. Navarra (eds) Analysis of Climate Variability: Applications of Statistical Techniques.

579   Springer-Verlag, Berlin, 11–26.

580 Walsby, A. E., A. Avery & F. Schanz, 1998. The critical pressures of gas vesicles in

581   *Planktothrix rubescens* in relation to the depth of winter mixing in Lake Zurich,

582   Switzerland. Journal of Plankton Research 20:1357-1375.

583 Walsby, A. E., Z. Dubinsky, J. C. Kromkamp, C. Lehmann & F. Schanz, 2001. The effects of

584   diel changes in photosynthetic coefficients and depth of *Planktothrix rubescens* on the

585   daily integral of photosynthesis in Lake Zurich. Aquatic Sciences 63:326-349.

586 Walsby, A. E., G. Ng, C. Dunn & P. A. Davis, 2004. Comparison of the depth where

587   *Planktothrix rubescens* stratifies and the depth where the daily insolation supports its

588   neutral buoyancy. New Phytologist 162:133-145.

589 Walsby, A. E. & F. Schanz, 2002. Light-dependent growth rate determines changes in the

590   population of *Planktothrix rubescens* over the annual cycle in Lake Zurich, Switzerland.

591   New Phytologist 154:671-687.

592 Weyhenmeyer, G. A., R. Adrian, U. Gaedke, D. M. Livingstone & S. C. Maberly, 2002.

593   Response of phytoplankton in European lakes to a change in the North Atlantic Oscillation.

594   Verhandlungen der Internationalen Vereinigung für Theoretische und Angewandte

595   Limnologie 28:1436-1439.

596 Winder, M. & D. E. Schindler, 2004. Climatic effects on the phenology of lake processes.

597   Global Change Biology 10:1844-1856.

598   Winder, M. & U. Sommer, 2012. Phytoplankton response to a changing climate.

599   Hydrobiologia 698:5-16.

600   Wuest, A. & A. Lorke, 2003. Small-scale hydrodynamics in lakes. Annual Review of Fluid

601   Mechanics 35:373-412.

602   Yue, S., P. Pilon, B. Phinney & G. Cavadias, 2002. The influence of autocorrelation on the

603   ability to detect trend in hydrological series. Hydrological Processes 16:1807-1829.

604   **Table 1**. Spearman's correlation analysis of *Planktothrix rubescens* start and end populations

605   (biomass between 0-20 m) versus metalimnion onset, duration and annual thickness.

	P. rubescens start (June) (tons)	*P. rubescens* end (November) (tons)
Onset (Julian days)	-0.43*	-0.38*
Duration (Julian days)	n.s.	n.s.
Annual thickness (m)	-	-0.48**

606   Significance levels: $p > 0.05$ (n.s.); $p < 0.05$ (*); $p < 0.01$ (**); $p < 0.001$ (***).

Figure legends

608 **Fig. 1.** Temperature profiles, thermal gradients between 1 m depth layers and binary image of

609 the metalimnion exemplified for the years 1981 (**a**, **b** and **c**) and 2000 (**d**, **e** and **f**). Details on

610 the determination of metalimnion boundaries are described in the text.

611 **Fig. 2.** Temperature trends between 1978 and 2013. Left: analyzed for each month of the

612 year; significant changes ($p < 0.05$, MK trend test) in air (top) and water (bottom)

613 temperatures ($n = 36$ per depth per month). Color bar shows correlation range (*tau* values).

614 Seasonal MK trend test was applied for the whole year data-set for each depth. Right: Range

615 of water temperature increase per depth where significant trends were detected. Bars range

616 from minimum to maximum. Points and dotted line depict mean values. Rightmost column:

617 month, in which the maximum increase per depth was found.

618 **Fig. 3.** Temporal dimensions (a) and mean duration (b) of the metalimnion between 1978 and

619 2013. Bar color code: 1978-1989 (blue), 1990-1999 (yellow), 2000-2013 (red). Black line:

620 linear trend according to Sen's slope estimation with confidence intervals for stratification

621 onset (dashed) and end in (a), and duration in (b). $p < 0.01$ (**).

622 **Fig. 4.** Spatial dimensions of the metalimnion between 1978 and 2013. (a) upper boundary,

623 (b) lower boundary, (c) mean thickness. Bar colors: significant positive (red) or negative

624 (blue) trend over time according to MK trend tests. (d) MK trend analysis with Sen's slope of

625 decreasing mean thickness of the metalimnion for July-August ($p < 0.001$) with confidence

626 intervals.

627 **Fig. 5.** Mean depth of *P. rubescens* biomass maxima (orange line) and neutral buoyancy

628 (green line) between June and September. Gray area depicts the mean metalimnion

629 boundaries for each month, black dotted line shows the center of the metalimnion. Years in

630 which *P. rubescens* biomass was below detection limit are indicated by black triangles on the

631 x-axis.

632   **Fig. 6.** Relationship between *P. rubescens* biomass in June and July (a), July and August (b),

633   and between metalimnetic center temperatures (Tmc) and *P. rubescens* biomass in July (c)

634   and August (d). Points colors: 1978-1979 (black), 1980-1989 (green), 1990-1999 (blue),

635   2000-2013 (red). Development of Tmc (1978-2013) for July (e) and August (f) according to

636   MK trend analysis. Linear trend according to Sen's slope estimates. Significance levels: $p >$

637   0.05 (ns), $p < 0.05$ (*), $p < 0.01$ (**), $p < 0.001$ (***).

638   **Supplementary Material**

639   **Five supporting figures composed in one pdf file (Yankova_Supplementary_FiguresS1-**

640   **S5.pdf)**

641   S1. Long-term data of the biomass (μg fresh-weight L^{-1}) of the cyanobacterium *Planktothrix*

642   *rubescens* in Lake Zurich, Switzerland. Black lines in each year show the upper and lower

643   boundaries of the metalimnion during thermal stratification.

644   S2. Annual air temperature deviations from the mean for the period 1978-2013 for each

645   month. Black lines: trend according to Sen's slope estimation. Significance levels: $p < 0.05$

646   (*), $p < 0.01$ (**), $p < 0.001$ (***).

647   S3. Sen's slope coefficients for significant trends (see Fig. 2) of water temperature (lines and

648   points) and air temperature (dashed lines; yellow: November, pink: May, red: June, green:

649   April) between 1978 and 2013.

650   S4. Comparison between Schmidt stability (*S*) thresholds and metalimnion onset (a),

651   termination (b) and duration (c). Red dashed line marks the highest agreement between both

652   approaches.

653   S5. Bray-Curtis dissimilarity analysis for the parameters: upper metalimnion boundary

654   (Upper), lower metalimnion boundary (Lower), metalimnion center (Center), depth of

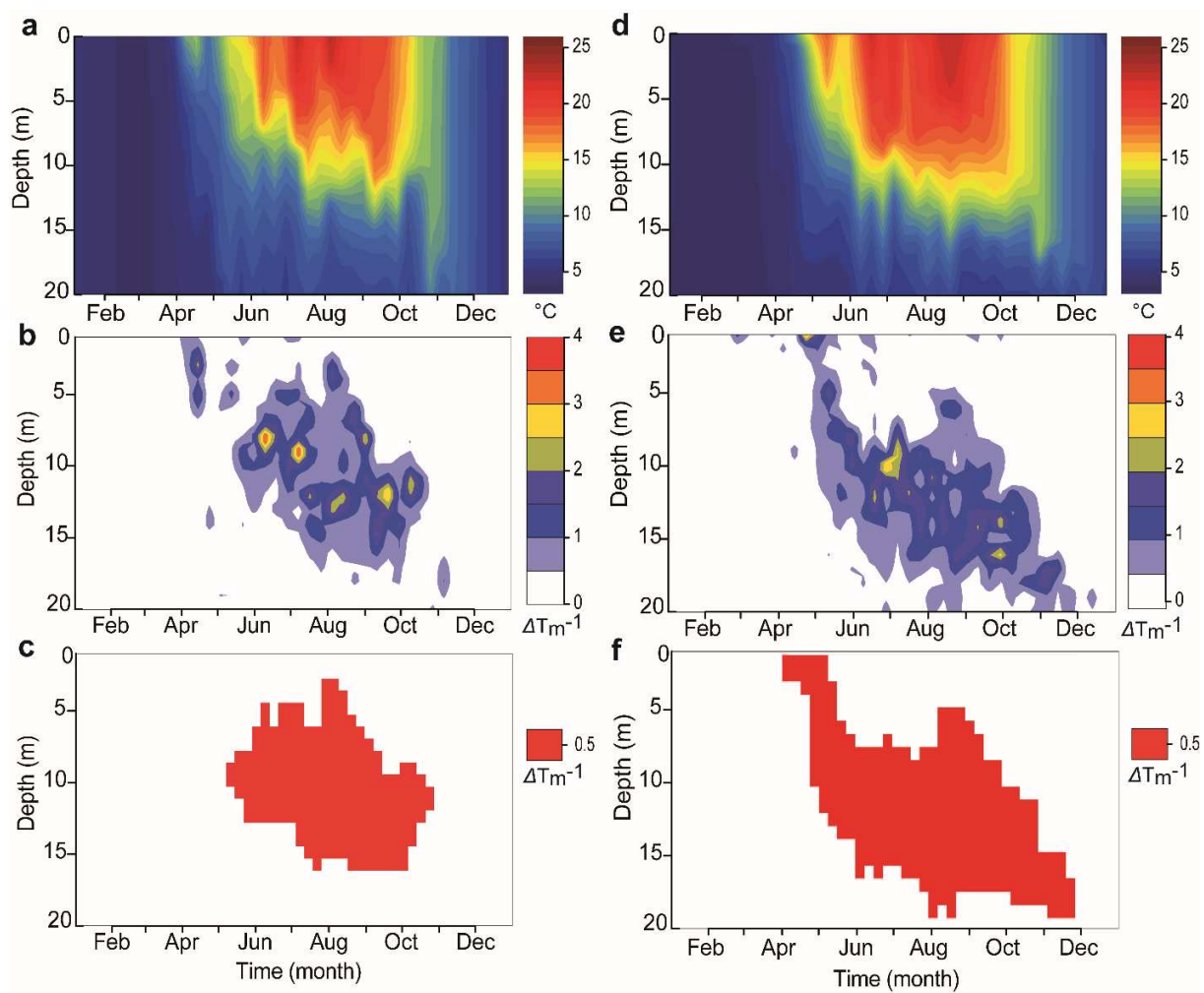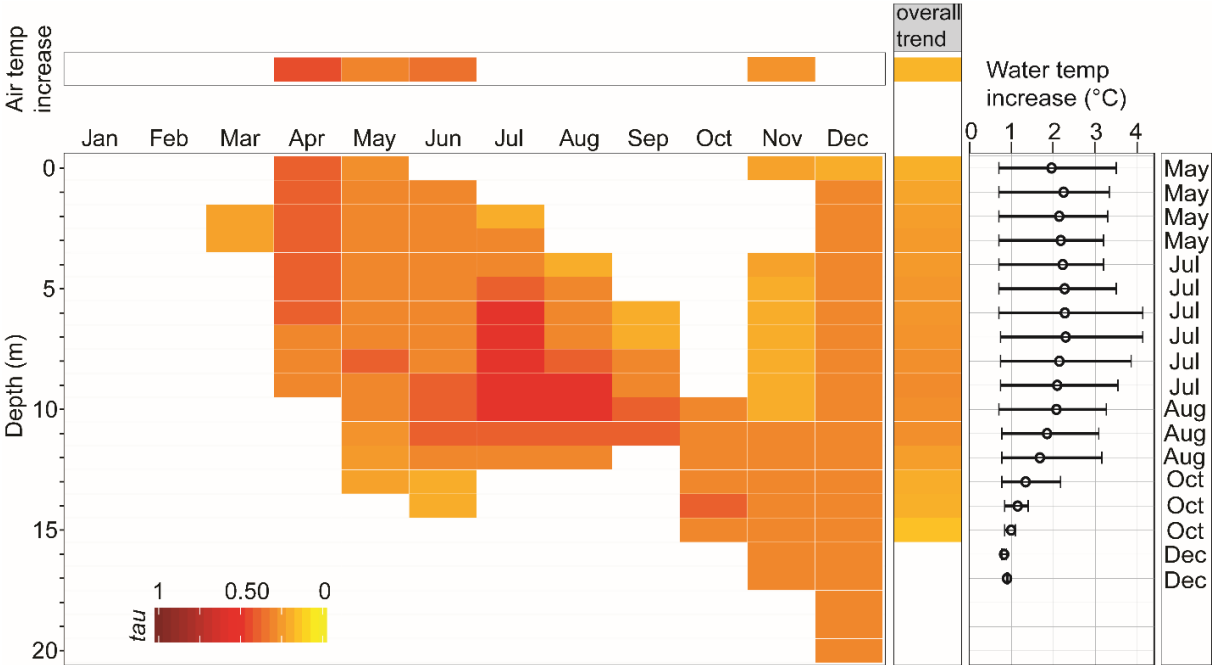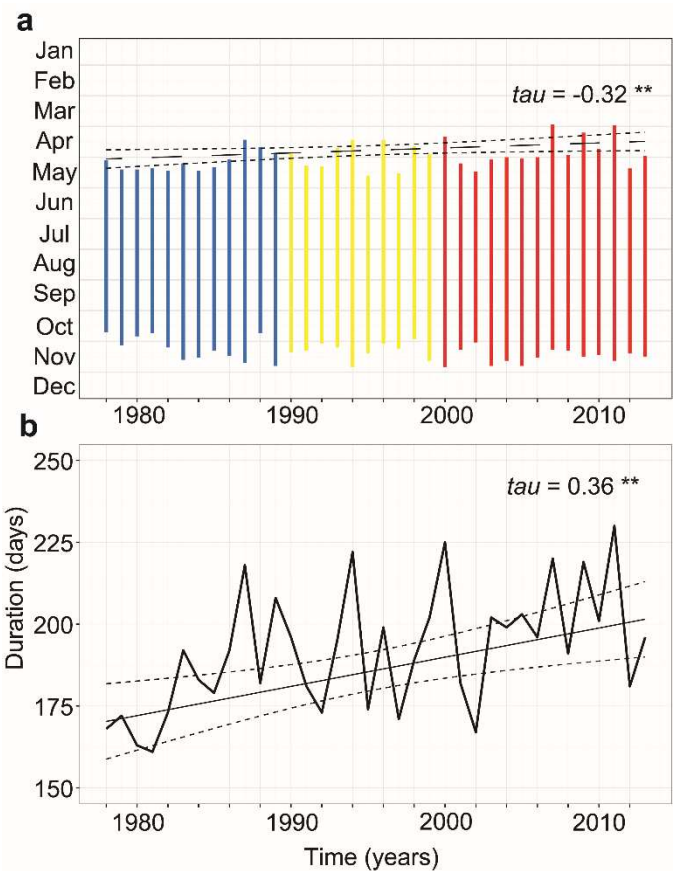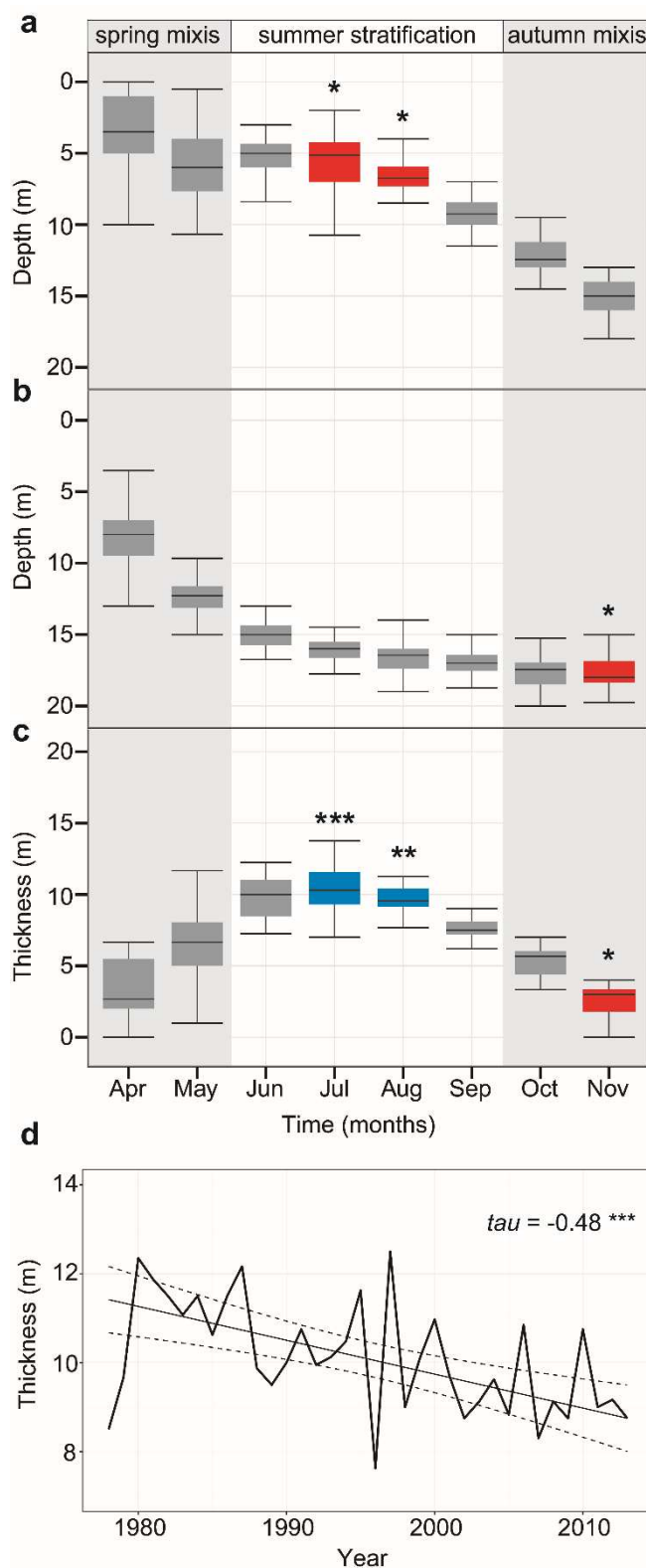655   maximum *P. rubescens* (Max *P.r.*) and neutral buoyancy depth (NB).

656

657

658

659

660   Fig. 1

670   Fig. 2

671

672

673

674

675

676

677

678

679

680

681

682

683   Fig. 3

698   Fig. 5

699

depth of max *P. rubescens* — neutral buoyancy depth — — metalimnion center
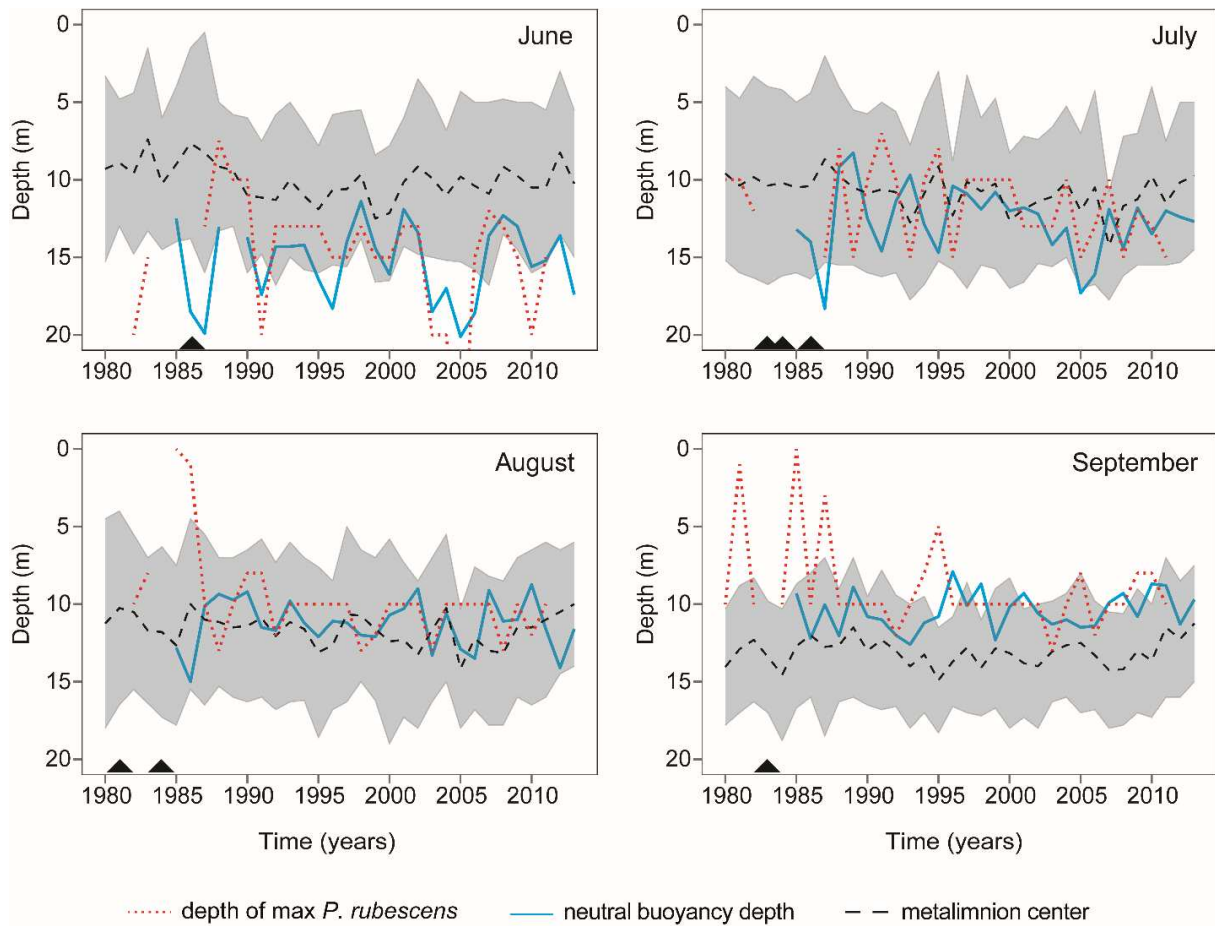
700

701

702

703

704

705

706

707

35

708   Fig. 6

709

710

711

712

713

714

715

716

717

718   Fig. S1

719

720

721

722

723   Fig. S2

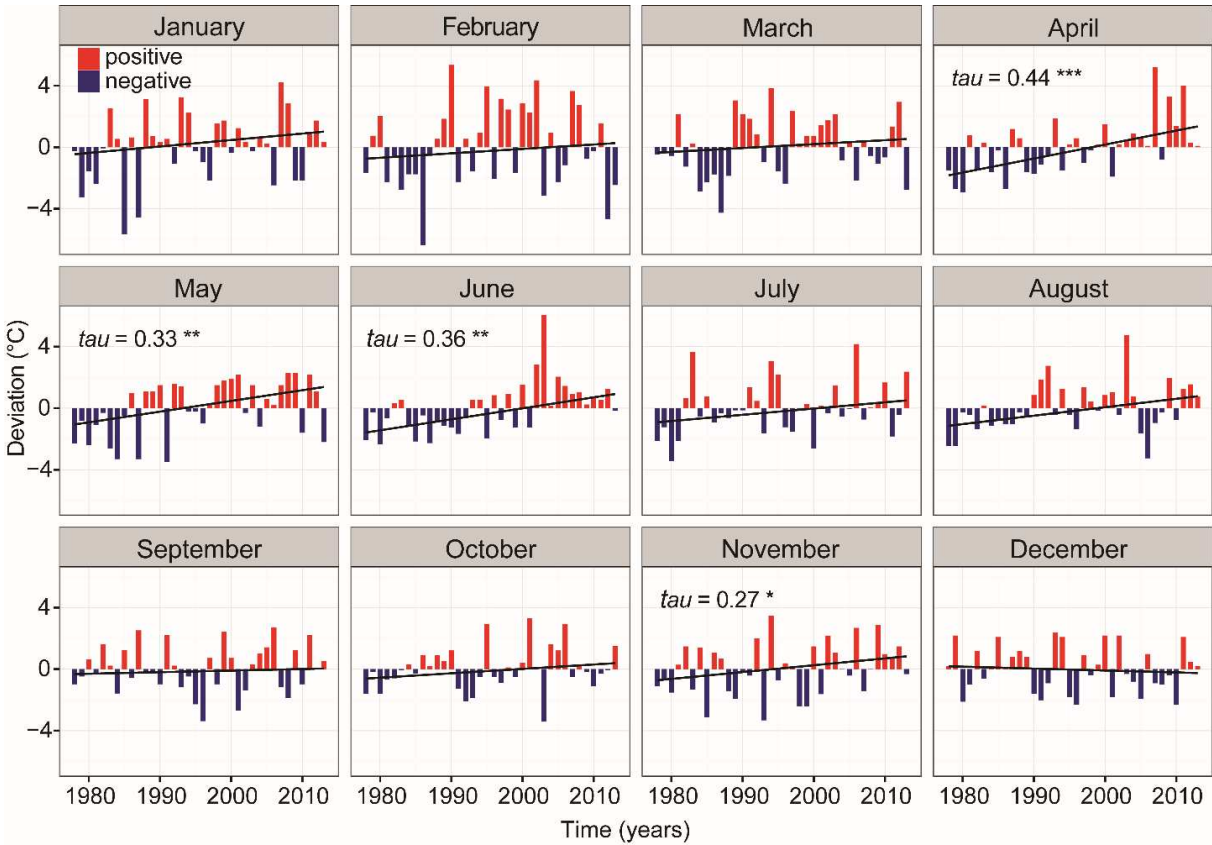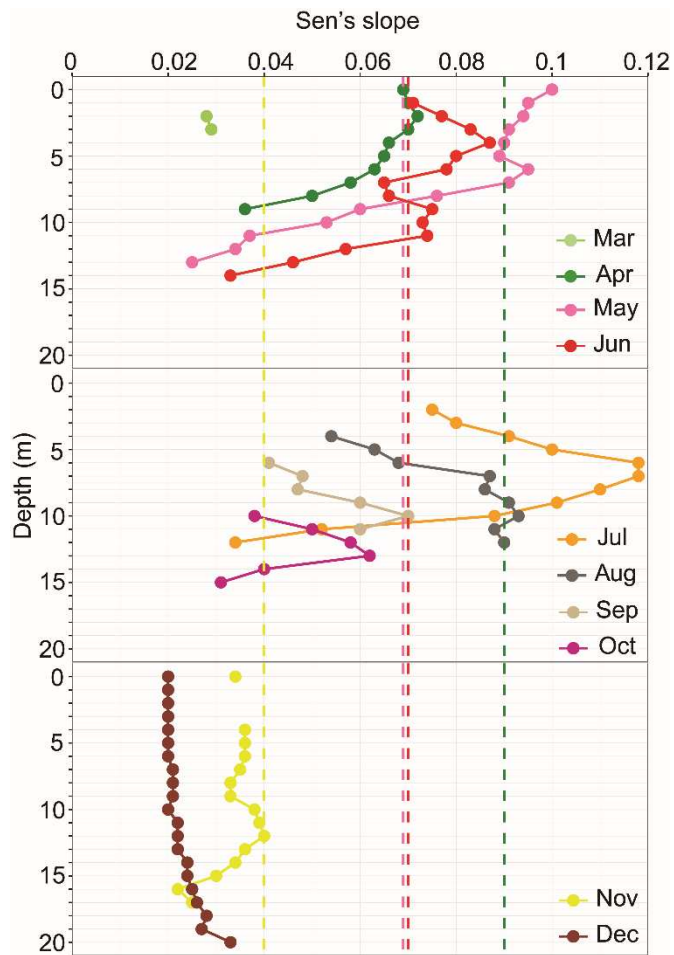724

725

726

727

728

729

730

731

732

733
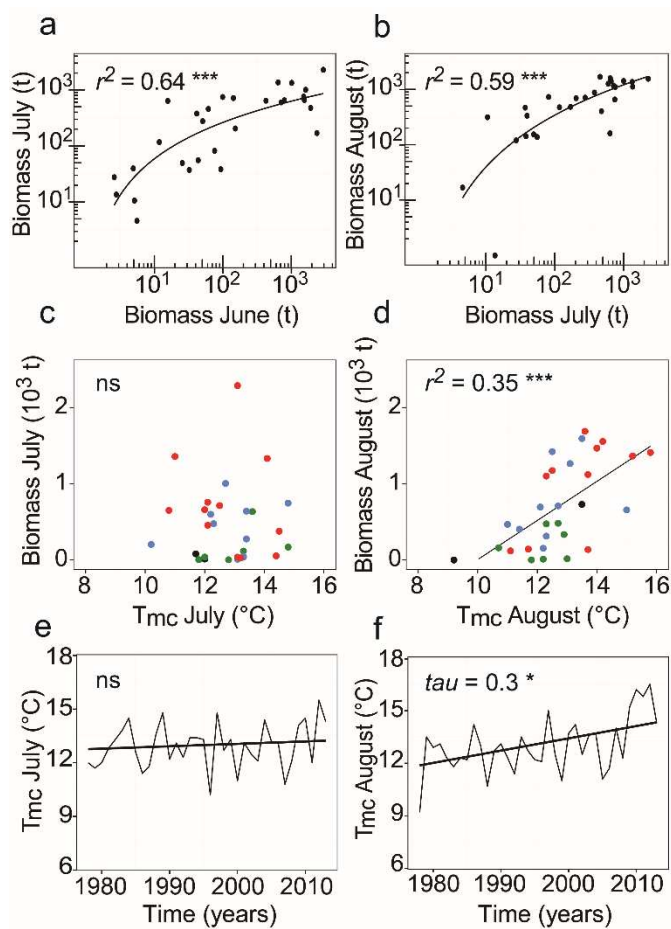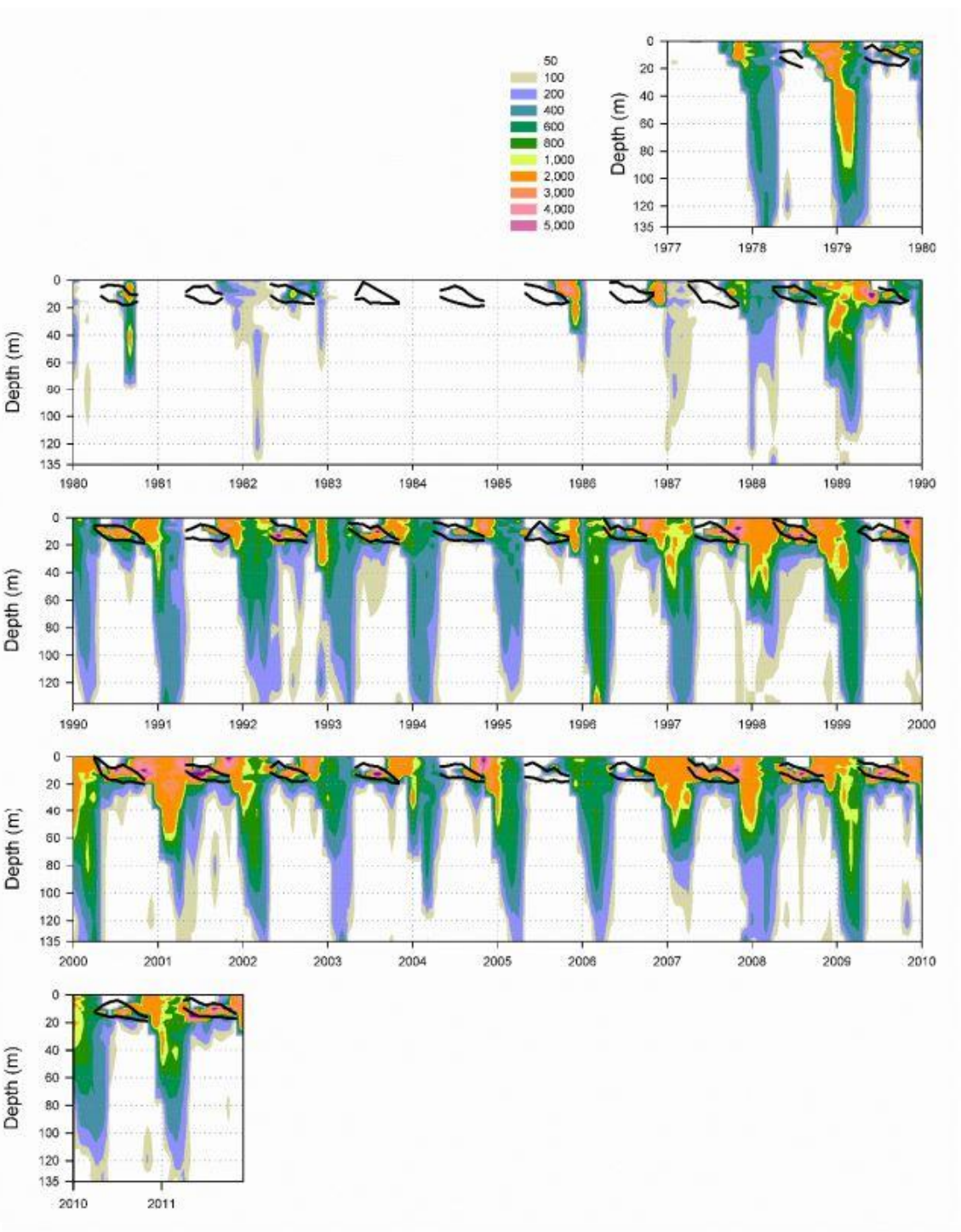
734   Fig. S3

735

736

737

738

739

740

741

742

743

744   Fig. S4

745

746

747

748

749

750

751

752   Fig. S5

Bray-Curtis dissimilarity index

753